

Sandwich-Type Electrochemiluminescence Immunosensor Based on CDs@dSiO₂ Nanoparticles as Nanoprobe and Co-Reactant

A-Ling Chen¹, Xiao-Yan Wang¹, Qing Zhang², Ning Bao³ and Shou-Nian Ding^{1,*}

- ¹ Jiangsu Province Hi-Tech Key Laboratory for Bio-medical Research, School of Chemistry and Chemical Engineering, Southeast University, Nanjing 211189, China
² Key Laboratory of Consumer Product Quality Safety Inspection and Risk Assessment for State Market Regulation, Chinese Academy of Inspection and Quarantine, Beijing 100176, China
³ School of Public Health, Nantong University, Nantong 226019, China
 * Correspondence: snding@seu.edu.cn

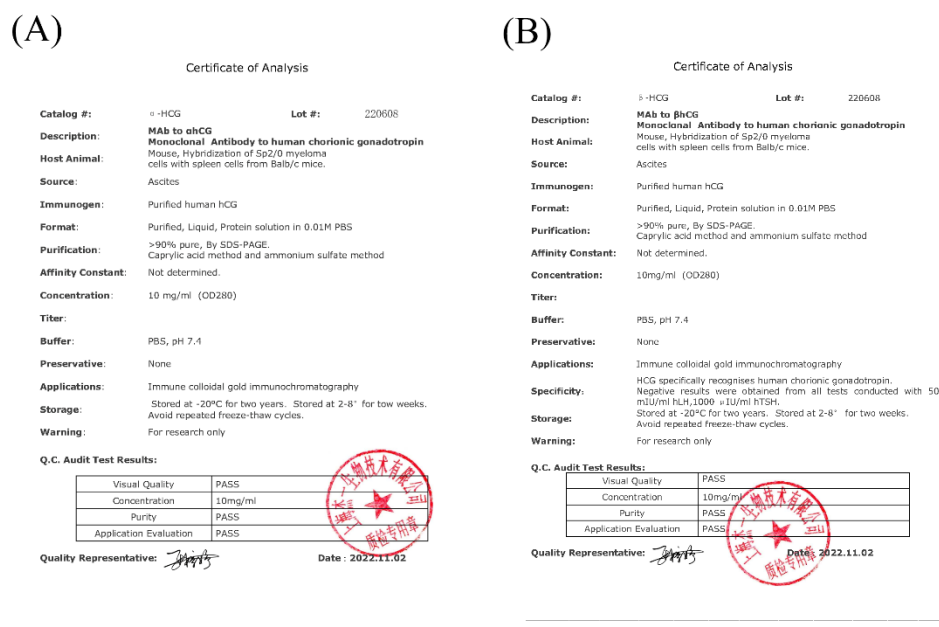


Figure S1. The certificate of analysis of HCG-Ab₁ and HCG-Ab₂.

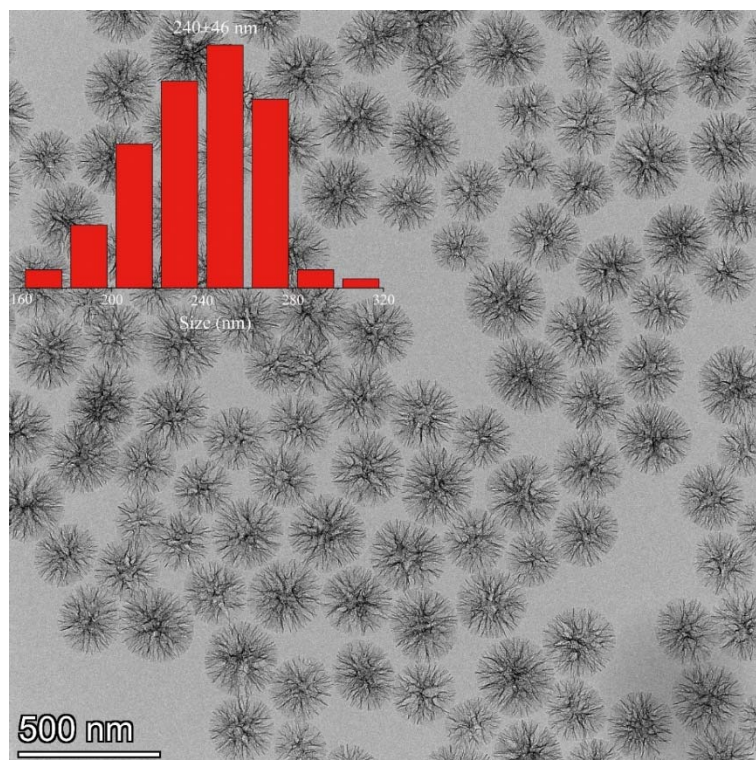


Figure S2. TEM image of dSiO₂ nanospheres at lower magnification. And the corresponding particle size distribution (insert).

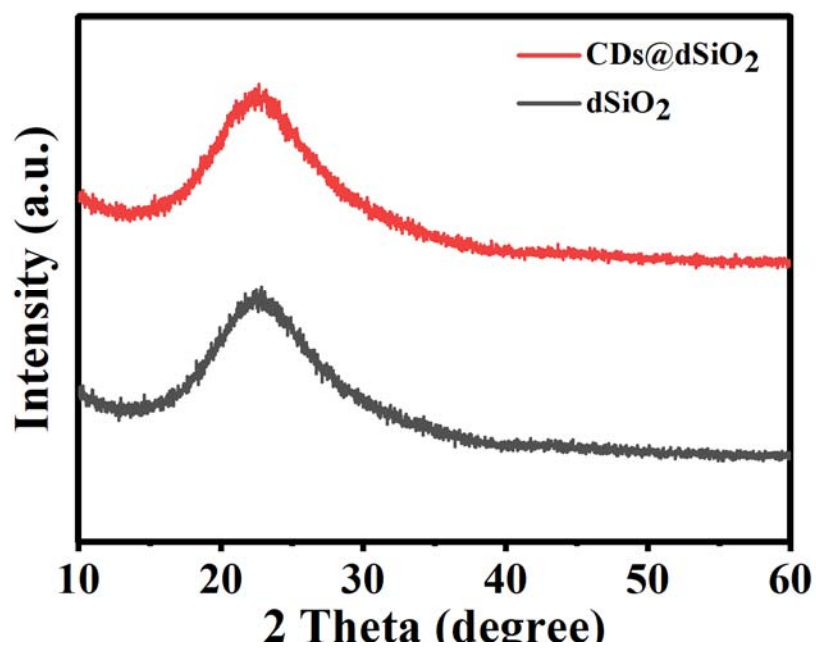


Figure S3. Powder X-ray Diffraction Pattern of dSiO₂ NPs (black curve) and CDs@dSiO₂ NPs (red curve).

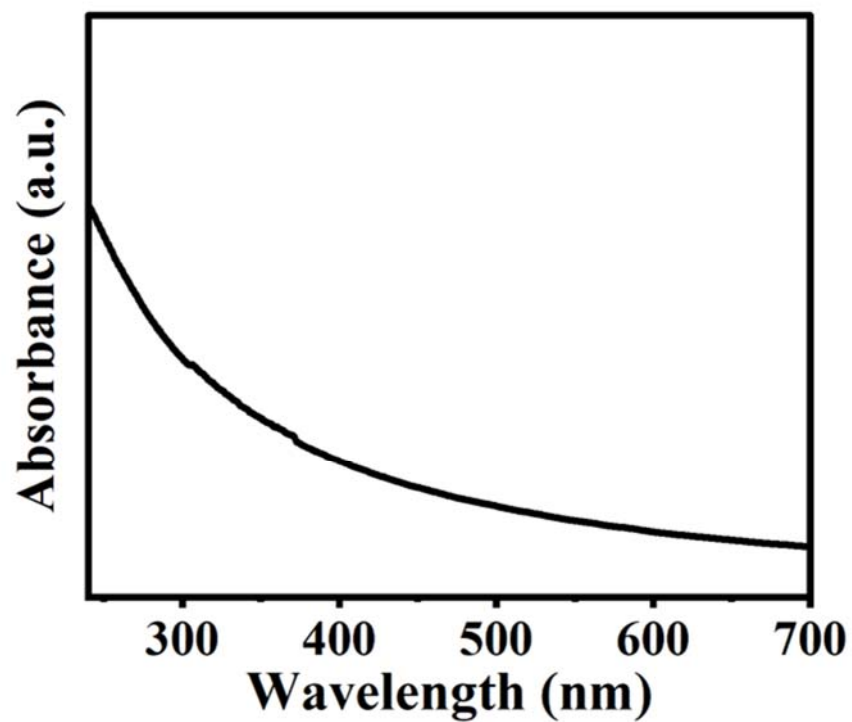


Figure S4. UV-vis absorption spectra of dSiO₂ NPs.

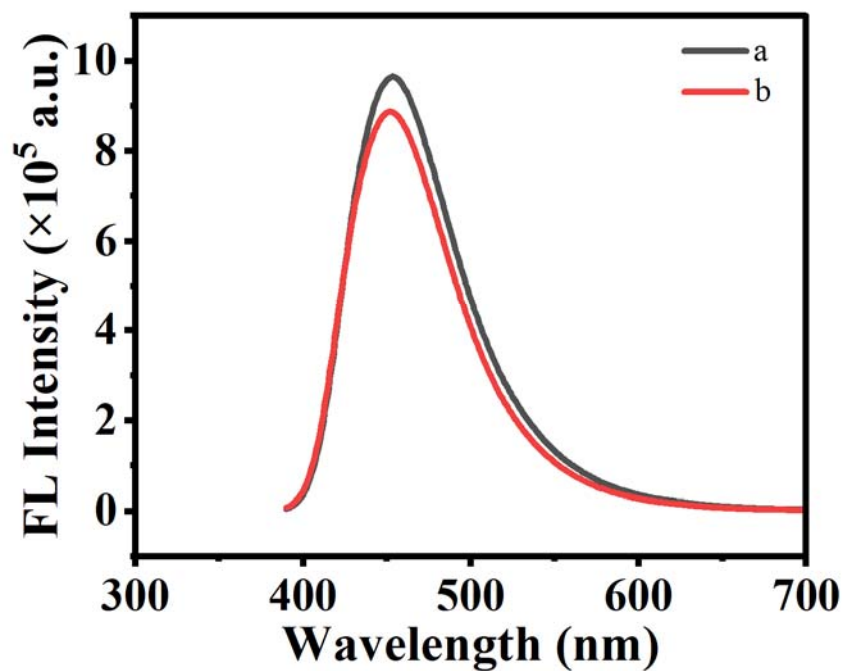


Figure S5. Fluorescence spectrum of (a) CDs and (b) residual CDs in supernatant.

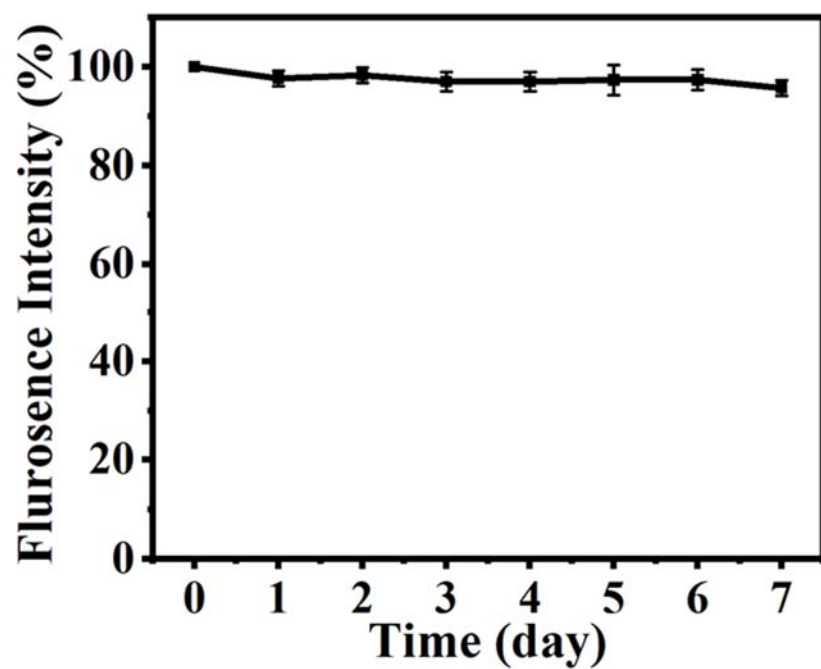


Figure S6. Fluorescent stabilities of CDs@dSiO₂ NPs against storage time.

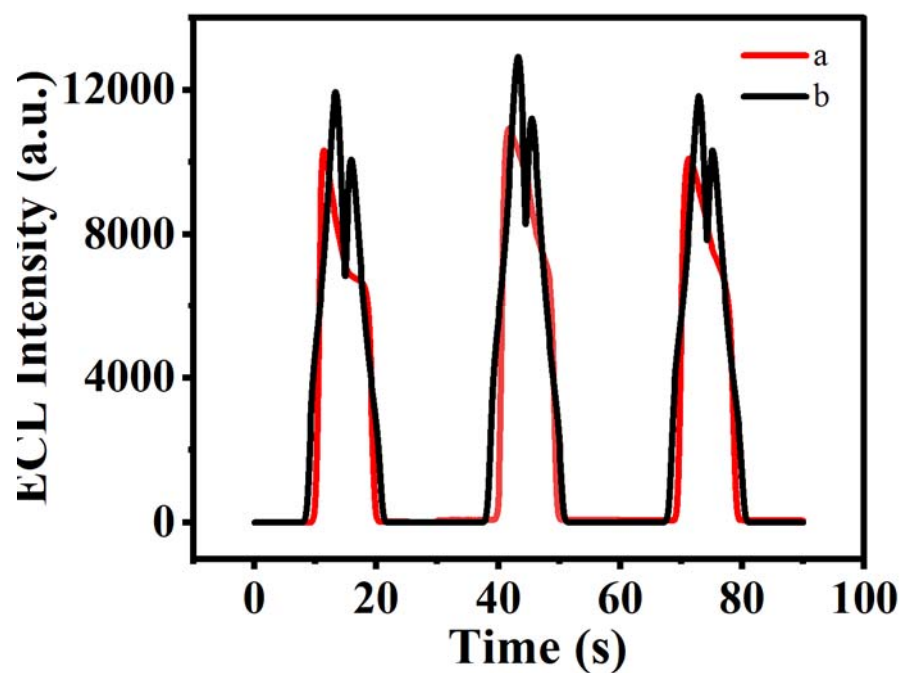


Figure S7. ECL curves of (a) CDs (15.62 mg/mL) and (b) TPrA (1.43 mg/mL) in the solution of 0.1 M PBS (pH = 7.4) containing 50 μ M Ru(bpy)₃²⁺. The voltage of PMT was set at 600 V.

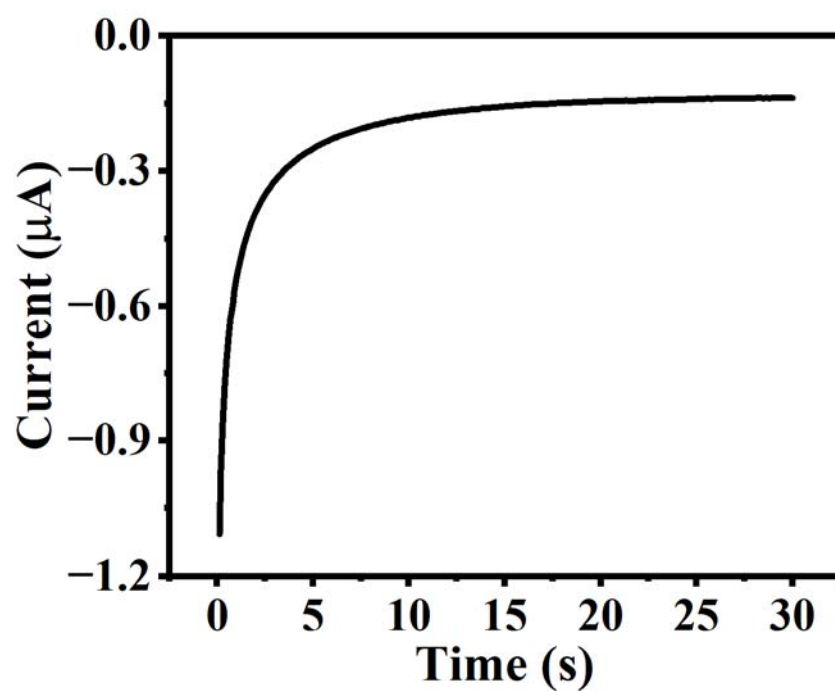


Figure S8. The current-time curve of electrodeposited Au NPs.

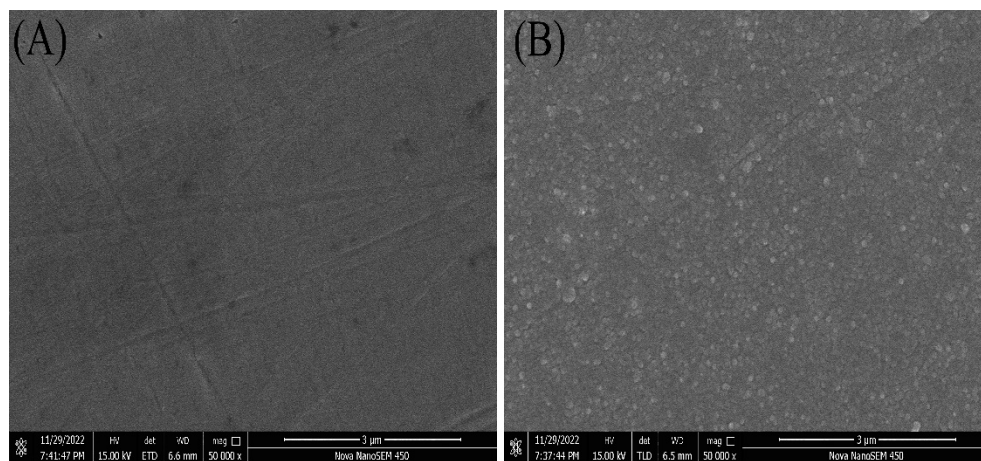


Figure S9. SEM image of electrode surface (A) GCE, (B) Au NPs-GCE.

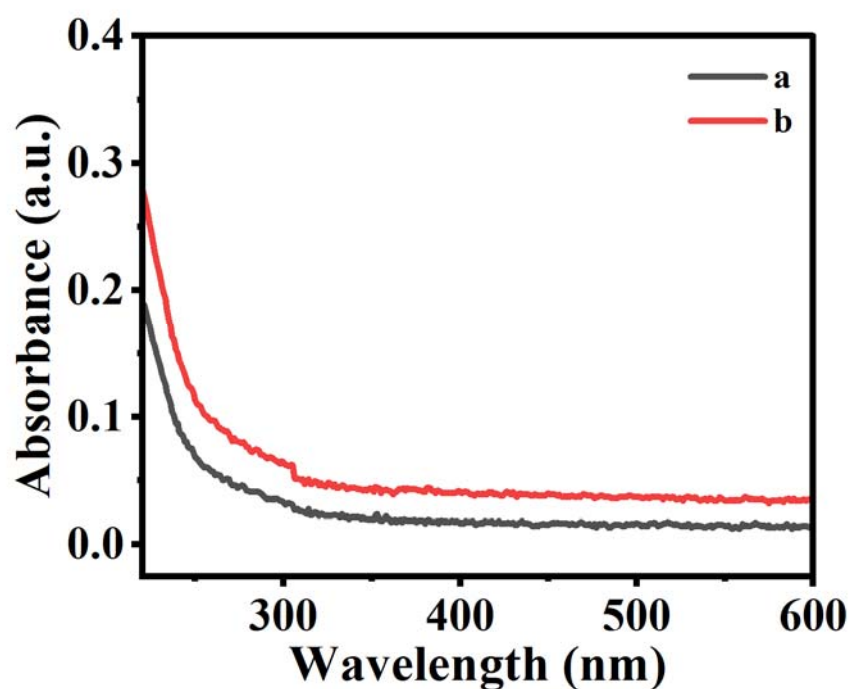


Figure S10. UV-vis absorption spectrum of (a) HCG-Ab₁ (0.016 mg/mL) and (b) a solution contains the excess HCG-Ab₁ of the constructed immunosensor.

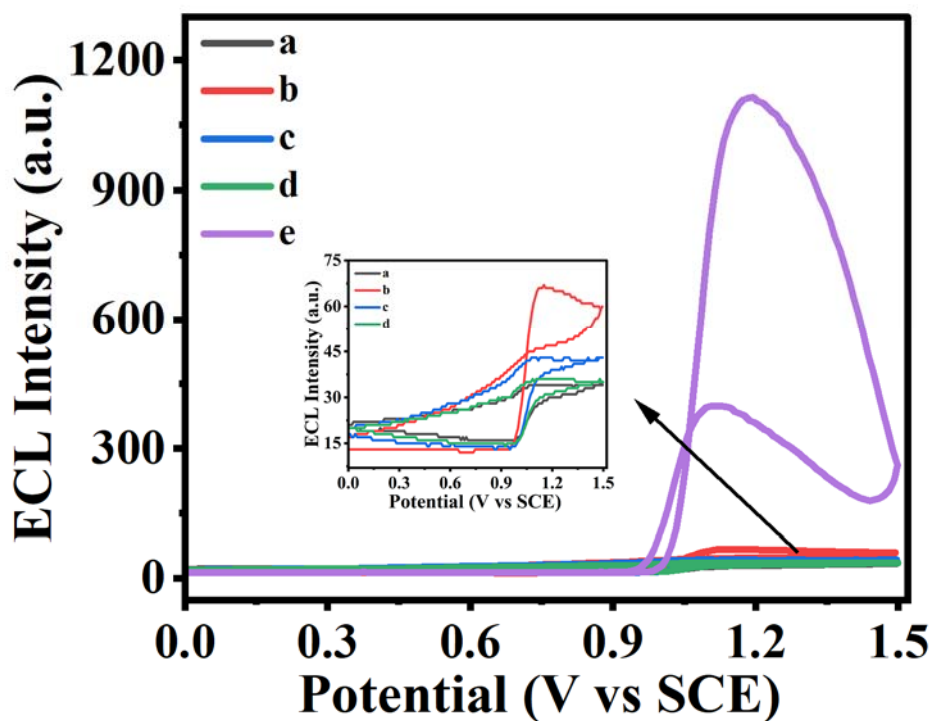


Figure S11. The ECL spectra of electrodes modified with different substances (a) GCE, (b) Ab₁/Au/GCE, (c) BSA/Ab₁/ Au/GCE, (d) Ag/ BSA/Ab₁/ Au/GCE and (e) Ab₂-CDs@dSiO₂ NPs / Ag/ BSA/Ab₁/ Au/GCE in a solution of 0.01 M PBS (pH = 7.4) containing 50 μ M Ru(bpy)₃²⁺. The voltage of PMT was set at 800 V.

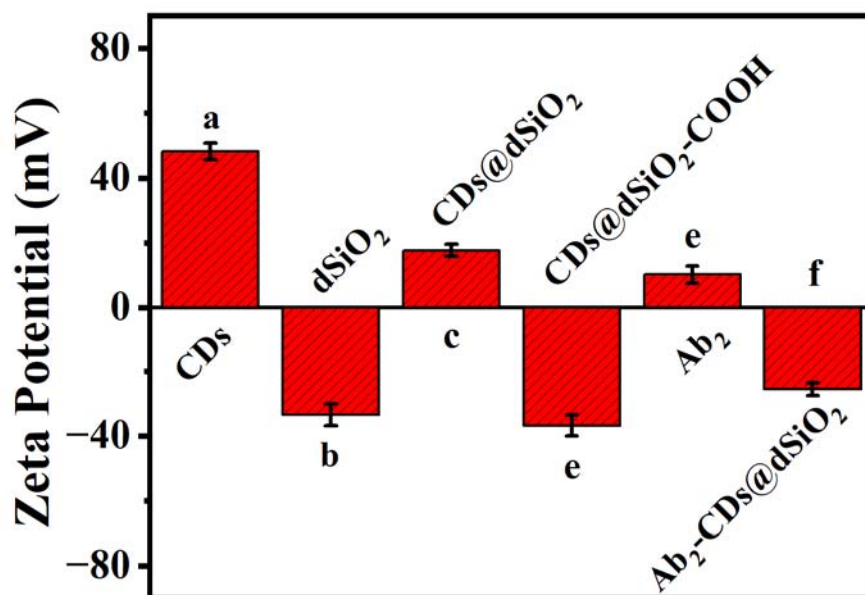


Figure S12. Zeta potential of (a) CDs, (b) dSiO₂, (c) CDs@dSiO₂, (d) CDs@dSiO₂-COOH, (e) Ab₂, and (f) CDs@dSiO₂-Ab₂ in the solution of 0.01 M PBS (pH = 7.4).

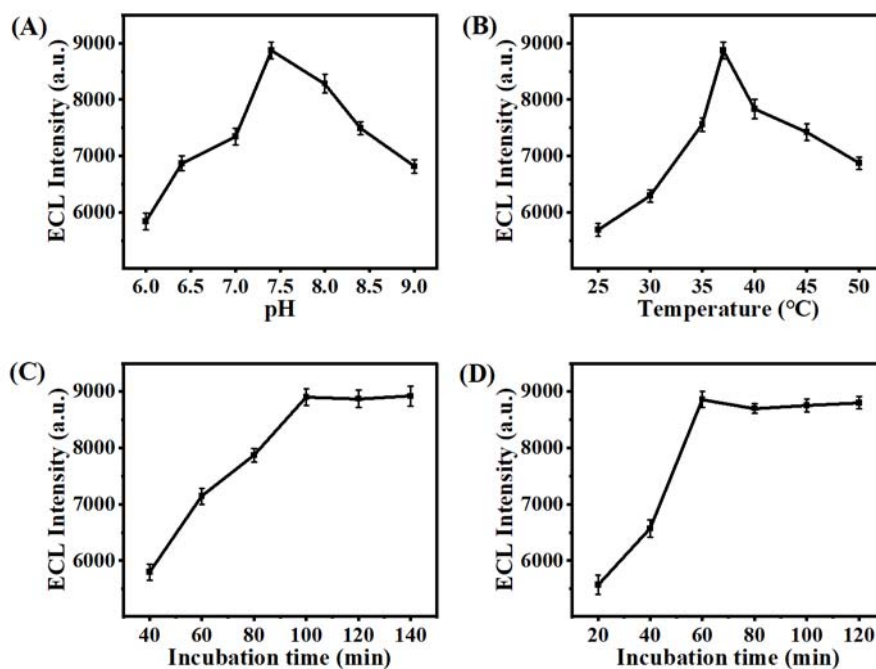


Figure S13. Optimization of (A) pH of PBS. (B) Incubation temperature. (C) Incubation time for Ab₁ bind to the electrode. (D) Specific binding time between the Ag and Ab₁. (Error bars: SD, n = 3). The voltage of PMT was set at 800 V.

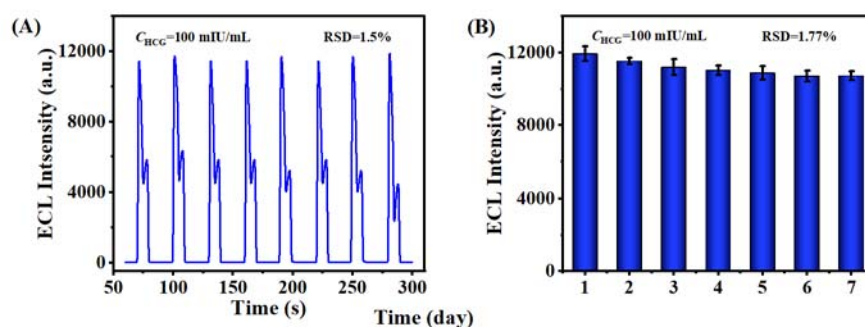


Figure S14. (A) Performance stability and (B) Storage stability of the ECL immunosensor. (Error bars: SD, n = 3). The voltage of PMT was set at 800 V.

Table S1. Comparison of analytical performances with other reported HCG bioassays.

Detection Method	Linear Range	Detection Limit	Ref.
Immunochromatographic strip	0.5-500 mIU/mL	0.22 mIU/mL	[1]
Surface-enhanced Raman scattering	0.5~200 mIU/mL	0.18 mIU/mL	[2]
Chemiluminescence	0.1~10 mIU/mL	0.06 mIU/mL	[3]
Electrochemiluminescence	0.001~500 mIU/mL	0.0003 mIU/mL	[4]
Electrochemiluminescence	0.001~500 mIU/mL	0.00033 mIU/mL	[5]
Electrochemiluminescence	0.0005~500 mIU/mL	0.00019 mIU/mL	Herein

Table S2. Analytical results for HCG detection in human serum specimens.

Sample	Initial Human Serum	Added (mIU/mL)	Measured (mIU/mL)	Average (mIU/mL)	RSD (%)	Recovery (n=3, %)
Serum 1	<LOD	5.00	4.48	5.72	4.4	100.1
			4.87			
			4.48			
Serum 2	<LOD	15.00	13.36	14.15	6.7	99.94
			13.88			
			15.20			
			24.4			
Serum 3	<LOD	25.00	25.87	25.43	2.3	100
			26.02			
			26.02			

References

- Wang, X.; Xue, C.H.; Yang, D.; Jia, S.T.; Ding, Y.R.; Lei, L.; Gao, K.Y.; Jia, T.T. Modification of a nitrocellulose membrane with nanofibers for sensitivity enhancement in lateral flow test strips. *Rsc Advances*. **2021**, *11*, 26493–26501. <https://doi.org/10.1039/d1ra04369b>.
- Wen, G.Q.; Liang, X.J.; Liu, Q.Y.; Liang, A.H.; Jiang, Z.L. A novel nanocatalytic SERS detection of trace human chorionic gonadotropin using labeled-free Vitoria blue 4R as molecular probe. *Biosens. Bioelectron.* **2016**, *85*, 450–456. <https://doi.org/10.1016/j.bios.2016.05.024>.
- Lei, J.; Jing, T.; Zhou, T.; Zhou, Y.; Wu, W.; Mei, S.; Zhou, Y. A simple and sensitive immunoassay for the determination of human chorionic gonadotropin by graphene-based chemiluminescence resonance energy transfer. *Biosens. Bioelectron.* **2014**, *54*, 72–77. <https://doi.org/10.1016/j.bios.2013.10.033>.
- Zhang, A.; Guo, W.W.; Ke, H.; Zhang, X.; Zhang, H.; Huang, C.S.; Yang, D.P.; Jia, N.Q.; Cui, D.X. Sandwich-format ECL immunosensor based on Au star@BSA-Luminol nanocomposites for determination of human chorionic gonadotropin. *Biosens. Bioelectron.* **2018**, *101*, 219–226. <https://doi.org/10.1016/j.bios.2017.10.040>.
- Qin, D.M.; Jiang, X.H.; Mo, G.C.; Zheng, X.F.; Deng, B.Y. Electrochemiluminescence immunoassay of human chorionic gonadotropin using silver carbon quantum dots and functionalized polymer nanospheres. *Microchim. Acta.* **2020**, *187*, 1–13. <https://doi.org/10.1007/s00604-020-04450-0>.